



Cite this: *Chem. Commun.*, 2020, **56**, 9667

Received 5th May 2020,  
Accepted 14th July 2020

DOI: 10.1039/d0cc03229h

[rsc.li/chemcomm](http://rsc.li/chemcomm)

**The soluble hydrogenase from *Ralstonia eutropha* provides an atom efficient regeneration system for reduced flavin cofactors using H<sub>2</sub> as an electron source. We demonstrated this system for highly selective ene-reductase-catalyzed C=C-double bond reductions and monooxygenase-catalyzed epoxidation. Reactions were expanded to aerobic conditions to supply H<sub>2</sub>O<sub>2</sub> for peroxygenase-catalyzed hydroxylations.**

Flavin mononucleotide (FMN) and flavin adenine dinucleotide (FAD) are key versatile cofactors for electron transfer and substrate conversion. Flavins are found as prosthetic groups in many biocatalysts including ene-reductases, monooxygenases, hydrogenases and oxidases. These flavoenzymes catalyze various industrially relevant reactions such as asymmetric hydrogenations and sulfoxidations, selective amine oxidations, and Baeyer–Villiger oxidations.<sup>1</sup>

In their reduced form (FNMH<sub>2</sub> and FADH<sub>2</sub>, respectively), flavins serve as electron donors for a broad range of biological redox reactions many of which are relevant in the organic synthesis.<sup>2</sup> In the case of preparative chemical applications (*i.e.*, biocatalysis), the stoichiometric reductant plays a crucial role in envisioning the economic feasibility and environmental impact of the reaction system. Mimicries of the natural, NAD(P)H-dependent regeneration pathways are currently the most widely used approach, but suffer from complex reaction schemes, the need for the nicotinamide cofactor and the formation of significant wastes originating from stoichiometric reductants such as glucose.<sup>3</sup> In addition, some photo<sup>4</sup> and electrochemical<sup>5,6</sup> approaches to regenerate reduced flavins have been reported.

<sup>a</sup> Institute of Chemistry, Technische Universität Berlin, Strasse des 17. Juni 135, 10623 Berlin, Germany. E-mail: [lars.lauterbach@tu-berlin.de](mailto:lars.lauterbach@tu-berlin.de)

<sup>b</sup> Department of Biotechnology, Delft University of Technology, Van der Maasweg 9, 2629HZ Delft, The Netherlands. E-mail: [f.hollmann@tudelft.nl](mailto:f.hollmann@tudelft.nl), [c.e.paul@tudelft.nl](mailto:c.e.paul@tudelft.nl)

† Electronic supplementary information (ESI) available: Details of H<sub>2</sub>-driven biotransformations; GC product analysis; kinetic parameters of SH for FMN and FAD; formation of H<sub>2</sub>O<sub>2</sub>. See DOI: 10.1039/d0cc03229h

## H<sub>2</sub> as a fuel for flavin- and H<sub>2</sub>O<sub>2</sub>-dependent biocatalytic reactions†

Ammar Al-Shameri, <sup>a</sup> Sébastien J.-P. Willot, <sup>b</sup> Caroline E. Paul, <sup>\*b</sup> Frank Hollmann <sup>\*b</sup> and Lars Lauterbach <sup>a</sup>

Hydrogen would be an ideal reductant, especially from an environmental point of view as it does not yield any waste-products and is sustainable when generated by electrolysis using renewable energy sources. The NAD<sup>+</sup>-reducing hydrogenase from *Ralstonia eutropha* (soluble hydrogenase, SH) uses molecular hydrogen (H<sub>2</sub>) to reduce NAD<sup>+</sup> to NADH and consists of a hydrogenase module (HoxHY) with a H<sub>2</sub> converting active site and a diaphorase module (HoxFUI<sub>2</sub>) with a NAD<sup>+</sup> binding site (Fig. 1).<sup>7–9</sup> H<sub>2</sub> is oxidized at the NiFe active site with three biologically untypical CN<sup>−</sup> and CO ligands. The electrons are transferred *via* the FMN-a close to the active site within the hydrogenase module and the Fe–S cluster chain to the second FMN-b at the NAD<sup>+</sup> binding site (Fig. 1). FMN-b serves here as a mediator between the one electron centers (Fe–S clusters) and the two-electron acceptor NAD<sup>+</sup>.<sup>10</sup> The flavins of the SH are non-covalently bound. During SH purification, FMN-a is easily lost and can be reconstituted by adding free FMN to the purified enzyme, which significantly improves the NAD<sup>+</sup> reduction activity.<sup>11,12</sup> Experiments with separately produced hydrogenase and diaphorase modules showed that the FMN-a of the hydrogenase module can be reconstituted under reducing conditions and the FMN-b of the diaphorase module is released under reducing conditions.<sup>8,9</sup> Purified SH shows a lag phase during activity, since most of the enzyme population is inactive and requires reverse electron transfer from NADH generated from an active enzyme population for reactivation.<sup>13,14</sup>

In contrast to most other hydrogenases, the SH is O<sub>2</sub> tolerant; *i.e.* its catalytic activity is not impaired by ambient O<sub>2</sub>.<sup>15</sup> SH has been employed for the recycling of NAD(P)H in various enzymatic reactions *in vitro* and *vivo*.<sup>16–18</sup> Compared with common NAD(P)H-regeneration systems such as formate dehydrogenase (generating CO<sub>2</sub> as a stoichiometric by-product) and glucose-6-phosphate dehydrogenase (yielding the corresponding gluconolactone), H<sub>2</sub>-driven cofactor recycling has the advantage of being 100% atom efficient, by-product-free and cheap since it only relies on H<sub>2</sub> as reductant.<sup>19,20</sup> Besides NAD<sup>+</sup>, SH is also known to reduce other electron acceptors such as ferricyanide, methylene blue and methyl viologen.<sup>13</sup> This catalytic



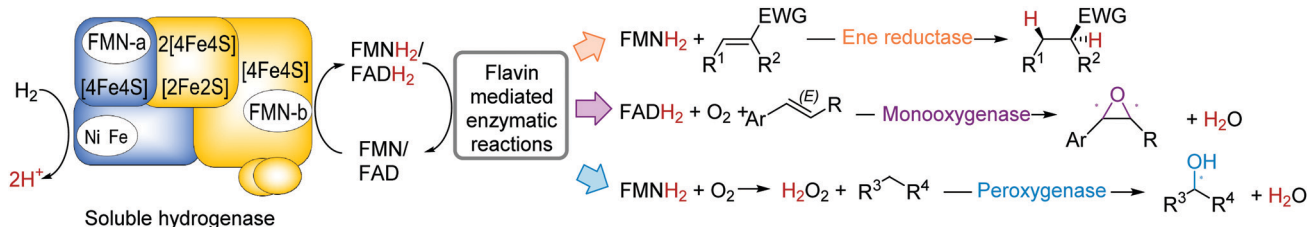


Fig. 1  $\text{H}_2$ -driven reduced flavin regeneration by soluble hydrogenase (SH) coupled with three biocatalysts to catalyze asymmetric hydrogenation, epoxidation and selective hydroxylation with high atomic efficiency. SH consists of a hydrogenase module (blue) with the NiFe active site responsible for  $\text{H}_2$  conversion and a diaphorase module (yellow) with the  $\text{NAD}^+$  binding site near FMN-b. Red H atoms show the fate of H atoms after  $\text{H}_2$  oxidation and illustrating the atom efficiency of  $\text{H}_2$ -driven flavin reduction. The resulted protons from  $\text{H}_2$  splitting are released to the solution and electrons are transferred via FMN-a, Fe-S clusters and FMN-b to the  $\text{NAD}^+$  binding site for FMN or FAD conversion to  $\text{FMNH}_2$  and  $\text{FADH}_2$ , respectively. Protons come from solution for flavin reduction. EWG = electron withdrawing group.

promiscuity in terms of electron acceptors may open up new avenues of  $\text{H}_2$ -driven biocatalysis while avoiding costly nicotinamide cofactors. We therefore evaluated SH-driven reduction of flavins to promote a range of biocatalytic redox reactions of synthetic interest.

First, we investigated the kinetic parameters for the SH-catalyzed reduction of FMN and FAD ( $\text{FADH}_2/\text{FAD}$  and  $\text{FMNH}_2/\text{FMN}$   $E^{\circ'} = -190$  mV) driven by  $\text{H}_2$  oxidation ( $\text{H}_2/2\text{H}^+ E^{\circ'} = -412$  mV), which is thermodynamically favoured. The specific activity of SH for reducing FMN was  $5.8 \text{ U mg}^{-1}$  ( $20.3 \text{ s}^{-1}$ ), with a  $K_{\text{m},\text{FMN}}$  of  $680 \mu\text{M}$  (Fig. S1, ESI†). Adding catalytic amounts of NADH increased the FMN specific activity by 100% and led to the disappearance of the lag phase. The disappearance of the lag phase is explained by faster reactivation under reducing conditions and reverse electron transfer (see above). Surprisingly, SH exhibited a significantly lower activity on FAD ( $0.14 \text{ U mg}^{-1}$ ,  $0.49 \text{ s}^{-1}$ ), which prohibited the precise determination of its  $K_{\text{m}}$  value. The higher activity towards the FMN compared with the longer FAD, as well as the increased FMN activity in the presence of NADH, support the reaction model, that the reduction occurs by temporarily substituting the prosthetic FMN-b by free flavin. After reduction of bound flavin, it is released again (Fig. 1). The FMN-b in the Rossmann fold is deeper submerged than the binding site of  $\text{NAD}^+$ , as seen in the crystal structure of the related SH from *Hydrogenophilus thermoluteolus*,<sup>21</sup> explaining the 17 times lower specific activities for FMN in comparison to  $\text{NAD}^+$  as the substrate.<sup>15</sup> The Fe-S clusters of the SH are buried in the protein matrix,<sup>21</sup> which may explain only a low contribution of Fe-S cluster in flavin reduction. The kinetic experiments demonstrated that SH-catalysed reduction of flavins is indeed feasible. Recently, the hydrogenase Hyd1 from *Escherichia coli* was described to catalyse the  $\text{H}_2$ -driven reduction of free flavins.<sup>22</sup> However, Hyd1 shows 180 times lower specific activity for FMN in comparison to SH and contains only additional Fe-S clusters and no flavins besides the NiFe active center. This supports the hypothesis that FMN-b of SH plays an important role for improved  $\text{H}_2$ -driven FMN reduction.

Encouraged by the high  $\text{H}_2$ -driven reduction activity of the SH, we explored the  $\text{H}_2$ -driven regeneration of reduced flavins to drive biocatalytic redox reactions (Fig. 1). As a first model reaction, we chose the stereoselective reduction of activated

$\text{C}=\text{C}$ -double bonds catalyzed by the ene reductase Old Yellow Enzyme from *Thermus scotoductus* (*TsOYE*).<sup>23</sup> In accordance with the substrate spectrum of *TsOYE*, a range of cyclic enones was reduced (Table 1).<sup>24</sup> Control reactions in the absence of either SH or  $\text{H}_2$  under otherwise identical conditions gave no detectable conversion. In particular, ketoisophorone was fully converted (99% conversion, Table 1, entry 1), albeit yielding a product with a significantly reduced optical purity (37%). Similar observations were made with this product and are generally associated with racemization under the reaction conditions (Table S3, ESI†). Interestingly, the control reaction without FMN

Table 1  $\text{H}_2$ -driven asymmetric reduction of alkenes

$\text{R}^1$	$\text{R}^2$	$\text{R}^3$	$\text{R}^4$	Product/mM	ee/%
Me	=O	H	$(\text{CH}_3)_2$	$21.8 \pm 0.4$	37 (R)
H	H	H	H	$9.7 \pm 0.2$	n.a.
Me	H	(S) isopropenyl	H	$1.9 \pm 0.2$	>99, 98.1 de (2R,5S)
Me	H	(R) isopropenyl	H	$1.1 \pm 0.1$	>99, 93.2 de (2R,5R)
Me	H	H	H	$17.8 \pm 0.5$	>94 (R)

Total turnover numbers<sup>a</sup>

<i>TsOYE</i>	SH	FMN
2625	8400	105

Reaction conditions: 2 mL of KPi buffer pH 7.5 containing:  $200 \mu\text{M}$  FMN,  $22 \text{ mM}$  substrate. The buffer was purged with  $\text{H}_2$  prior to adding the substrate, SH ( $2.5 \mu\text{M}$ ) and *TsOYE* ( $8 \mu\text{M}$ ). The reaction was performed at  $30^\circ\text{C}$  for 4–16 hours. Maximum products yields are indicated. Conversions and ee values were determined by GC-FID analysis. n.a. = not applicable. SH =  $\text{NAD}^+$ -reducing hydrogenase, *TsOYE* = ene reductase. <sup>a</sup> Total turnover numbers of mol 2-methylcyclohexanone per mol enzyme or cofactor were determined at end of experiment.



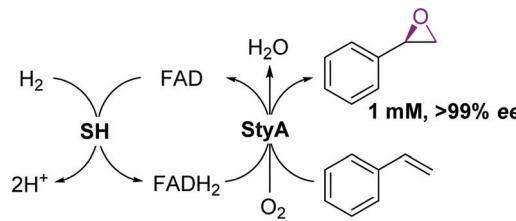
gave a low but detectable conversion, which may be indicative of a slow, direct electron transfer from SH to the flavin prosthetic group in *TsOYE*.<sup>25</sup> Pleasingly, already under non-optimized conditions, significant catalytic performances for both SH and FMN with TTN up to 8400 and 105, respectively, were observed (Table 1).

In order to demonstrate the  $O_2$  tolerance of the SH for flavin regeneration and the extension to the FAD cofactor, we used our system to drive the epoxidation of styrenes catalyzed by styrene monooxygenase from *Pseudomonas* sp. VLB120.<sup>26</sup> Styrene monooxygenase is a two-component, flavin monooxygenase composed of StyA, the FADH<sub>2</sub>-dependent monooxygenase subunit and StyB (a flavin reductase catalyzing the *in situ* generation of FADH<sub>2</sub> from FAD and NADH).<sup>27</sup> The FADH<sub>2</sub> regeneration system proposed here circumvents the nicotinamide cofactor together with the reductase subunit (StyB). Up to 1 mM of enantiopure (*S*)-styrene oxide was obtained upon incubation of StyA with SH and FAD under  $O_2/H_2$  atmosphere for the reduction of styrene with the co-substrate  $O_2$  (Scheme 1). The TTN of SH for FAD reduction was up to 333.

One major side reaction of the  $H_2$ -driven styrene epoxidation reaction was the oxidative uncoupling of the FADH<sub>2</sub> regeneration from the StyA-catalyzed epoxidation reaction. Due to the high reactivity of reduced flavin species with  $O_2$ , the StyA-related formation of 4a-hydroperoxoflavin yielding the desired epoxidation product competes with the spontaneous aerobic reoxidation of FADH<sub>2</sub> yielding  $H_2O_2$ .<sup>28</sup> Although this 'Oxygen Dilemma' severely impedes the StyA-catalyzed epoxidation reaction,<sup>29</sup> it is a promising approach to promote selective oxyfunctionalization reactions catalyzed by peroxygenases (UPOs). While UPOs rely on  $H_2O_2$  as a stoichiometric oxidant, they are also rapidly inactivated in the presence of excess amounts of  $H_2O_2$ , thereby necessitating precise control over the *in situ*  $H_2O_2$  concentration.<sup>30</sup> We therefore coupled the proposed SH-based flavin reduction system to the recombinant peroxygenase from *Agrocybe aegerita* (rAaeUPO) for selective hydroxylation reactions (Scheme 2 and Fig. S2, ESI†).<sup>31,32</sup>

To minimize evaporative loss of the volatile reagents under the non-optimized reaction conditions for the proof-of-concept, we utilized the two liquid phase approach (*i.e.*, applying the substrate as a neat organic layer to the aqueous reaction mixture). Under these conditions, 1.5 mM of enantiopure (*R*)-1-phenylethanol was obtained from ethylbenzene. The overall robustness of the reaction process needed to be improved, as the reaction typically ceased after 1 h. We attributed this short reaction time to the poor stability of SH in the presence of hydrophobic solvents,<sup>33</sup> which could be alleviated by immobilization of the biocatalyst as demonstrated previously.<sup>34</sup> Hence, we were pleased to observe that using 95 nM of the Amberlite FPA54 immobilized SH under identical conditions resulted in an accumulation of 4.4 mM of the enantiomerically pure product. Under these conditions (substituting ethylbenzene with cyclohexane), up to 3.7 mM of cyclohexanol product were obtained (Scheme 2 and Table S4, ESI†). Notably, the TTN for SH increased from 750 to approximately 46 000.

In air,  $H_2$  has a flammability range of 4–74% and can be explosive at concentrations of 19–57%.<sup>35</sup> An undesired combustion



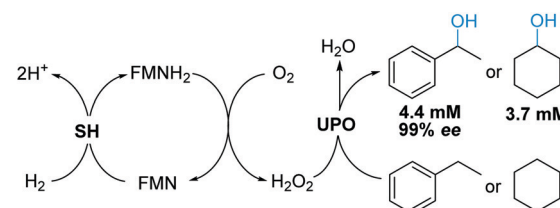
Total turnover numbers<sup>a</sup>

StyA	SH	FAD
200	333	3.3

**Scheme 1**  $H_2$ -driven asymmetric epoxidation of styrene. Reaction conditions: 1 mL of KPi buffer pH 7.5 containing 300  $\mu$ M FAD, 5 mM substrate. The gas mixture was 10%  $O_2$  30%  $N_2$  and 60%  $H_2$ . SH (3  $\mu$ M) and styrene monooxygenase (5  $\mu$ M) was added to start the reaction. The reaction was performed at 30 °C for 16 hours. Conversions and ee values were determined by GC-FID analysis. SH = NAD<sup>+</sup>-reducing hydrogenase, StyA = styrene monooxygenase. <sup>a</sup>Total turnover numbers of mol styrene epoxide per mol enzyme or cofactor.

during  $H_2$  driven catalysis can be prevented with mixtures that are very dilute in either  $H_2$  or  $O_2$ . As the SH has a  $K_M$  for  $H_2$  in the lower  $\mu$ M range,<sup>36</sup> this usually does not present a problem. Recently we developed a scalable platform that employs electrolysis to power biotransformations.<sup>37</sup> For  $H_2$  driven flavin reactions, a similar setup could be used in future studies. The supply of the right amount of  $H_2$  by electrolysis, which is continuously oxidized by the SH, would ensure a safe  $H_2$  handling by avoiding the formation of explosive gas mixtures.<sup>37</sup>

In conclusion, we have demonstrated as a proof of concept the  $H_2$ -driven reduction of flavins to promote selective biocatalytic reduction and oxidation reactions. The presented flavin recycling by  $H_2$  oxidation enabled the efficient reduction of activated alkenes, selective hydroxylation of alkanes and asymmetric epoxidation of styrene. The cofactor regeneration by a



Total turnover numbers<sup>a</sup>

UPO	SH	FMN
11250	750	225

46000 (immobilized)

**Scheme 2**  $H_2$ -driven hydroxylation of ethylbenzene and cyclohexane. Reaction conditions: 750  $\mu$ L of KPi buffer pH 7.5 containing 200  $\mu$ M FMN was added to 750  $\mu$ L of pure substrate in a two-phase system. The reaction was performed in pressure secured closed vials with 7 mL excess of headspace filled with gas composed of 40%  $O_2$  and 60%  $H_2$ . The reaction was performed at 30 °C for 4 hours. Sampling was taken from the organic phase. 95 nM of immobilized SH on 210 mg Amberlite<sup>TM</sup> FPA54 and 4  $\mu$ M UPO were added to start the reaction. Conversions and ee values were determined by GC-FID analysis. SH = NAD<sup>+</sup>-reducing hydrogenase, UPO = unspecific peroxygenase. <sup>a</sup>Total turnover numbers of mol ethylbenzene per mol enzyme or cofactor.



hydrogenase resulted in 100% atom efficiency without by-products, with a high turnover rate of up to  $20.3\text{ s}^{-1}$  and a total turnover number of up to 46 000. The electron delivery strategy circumvents NAD(P)H as the reductant and shortens previous multi-protein systems with reductases to a two-enzyme system. The  $\text{O}_2$  tolerance of the hydrogenase allowed aerobic reactions with a monooxygenase, whereas the spontaneous aerobic reoxidation of  $\text{FMNH}_2$  to  $\text{H}_2\text{O}_2$  fueled peroxygenase-catalyzed hydroxylation reactions. The general applicability of the NAD(P)H-free,  $\text{H}_2$ -driven flavin regeneration system was demonstrated using different oxidoreductases (*TsOYE*, *StyA* and *UPO*) and substrates (e.g., 2-methylcyclohexenone, styrene, ethylbenzene). The ability to use  $\text{H}_2$  as a fuel for flavin recycling opens up opportunities for highly atom-efficient biocatalysis, providing a versatile platform for future biotransformations with flavin- and  $\text{H}_2\text{O}_2$ -dependent enzymes.

A. A.-S. and L. L. received funding from the German Research Foundation (Deutsche Forschungsgemeinschaft, DFG, project number 284111627) and the Einstein foundation. Funded by the Deutsche Forschungsgemeinschaft (DFG, German Research Foundation) under Germany's Excellence Strategy – EXC 2008 – 390540038 – UniSysCat and by the Fonds der Chemischen Industrie. We thank Oliver Lenz for generous support by using his lab equipment, Changzhu Wu (University of Southern Denmark) for his support in providing Amberlite FPA54, and Ewald Jongkind (TU Delft) for his GC sampling assistance. We thank the Netherlands Organization for Scientific Research for financial support through a VICI grant (no. 724.014.003).

## Conflicts of interest

There are no conflicts to declare.

## Notes and references

- 1 G. de Gonzalo and M. W. Fraaije, *ChemCatChem*, 2013, **5**, 403–415.
- 2 E. Romero, J. R. Gómez Castellanos, G. Gadda, M. W. Fraaije and A. Mattevi, *Chem. Rev.*, 2018, **118**, 1742–1769.
- 3 W. Zhang and F. Hollmann, *Chem. Commun.*, 2018, **54**, 7281–7289.
- 4 L. Schmermund, V. Jurkaš, F. F. Özgen, G. D. Barone, H. C. Büchsenschütz, C. K. Winkler, S. Schmidt, R. Kourist and W. Kroutil, *ACS Catal.*, 2019, **9**, 4115–4144.
- 5 F. Hollmann, K. Hofstetter, T. Habicher, B. Hauer and A. Schmid, *J. Am. Chem. Soc.*, 2005, **127**, 6540–6541.
- 6 R. Ruinatscha, C. Dusny, K. Buehler and A. Schmid, *Adv. Synth. Catal.*, 2009, **351**, 2505–2515.
- 7 L. Lauterbach, O. Lenz and A. Vincent Kylie, *FEBS J.*, 2013, **280**, 3058–3068.
- 8 L. Lauterbach, Z. Idris, K. A. Vincent and O. Lenz, *PLoS One*, 2011, **6**, e25939.
- 9 L. Lauterbach, J. Liu, M. Horch, P. Hummel, A. Schwarze, M. Haumann, A. Vincent Kylie, O. Lenz and I. Zebger, *Eur. J. Inorg. Chem.*, 2011, 1067–1079.
- 10 M. Horch, L. Lauterbach, O. Lenz, P. Hildebrandt and I. Zebger, *FEBS Lett.*, 2012, **586**, 545–556.
- 11 K. Schneider and H. G. Schlegel, *Biochem. Biophys. Res. Commun.*, 1978, **84**, 564–571.
- 12 E. van der Linden, B. W. Faber, B. Bleijlevens, T. Burgdorf, M. Bernhard, B. Friedrich and S. P. Albracht, *Eur. J. Biochem.*, 2004, **271**, 801–808.
- 13 K. Schneider and H. G. Schlegel, *Biochim. Biophys. Acta*, 1976, **452**, 66.
- 14 T. Burgdorf, O. Lenz, T. Bührke, E. van der Linden, A. K. Jones, S. P. J. Albracht and B. Friedrich, *J. Mol. Microbiol. Biotechnol.*, 2005, **10**, 181–196.
- 15 L. Lauterbach and O. Lenz, *J. Am. Chem. Soc.*, 2013, **135**, 17897–17905.
- 16 A. Al-Shameri, N. Borlinghaus, L. Weinmann, P. Scheller, B. M. Nestl and L. Lauterbach, *Green Chem.*, 2019, **21**, 1396–1400.
- 17 T. H. Lonsdale, L. Lauterbach, S. Honda Malca, B. M. Nestl, B. Hauer and O. Lenz, *Chem. Commun.*, 2015, **51**, 16173–16175.
- 18 A. K. Holzer, K. Hiebler, F. G. Mutti, R. C. Simon, L. Lauterbach, O. Lenz and W. Kroutil, *Org. Lett.*, 2015, **17**, 2431–2433.
- 19 J. Ratzka, L. Lauterbach, O. Lenz and M. B. Ansorge-Schumacher, *Biocatal. Biotransform.*, 2011, **29**, 246–252.
- 20 L. Lauterbach and O. Lenz, *Curr. Opin. Chem. Biol.*, 2019, **49**, 91–96.
- 21 Y. Shomura, M. Taketa, H. Nakashima, H. Tai, H. Nakagawa, Y. Ikeda, M. Ishii, Y. Igarashi, H. Nishihara, K.-S. Yoon, S. Ogo, S. Hirota and Y. Higuchi, *Science*, 2017, **357**, 928–932.
- 22 S. J. Srinivasan, S. E. Cleary, C. E. Paul, M. A. Ramirez and K. A. Vincent, *ChemRxiv*, 2020, DOI: 10.26434/chemrxiv.12213398.
- 23 D. J. Opperman, L. A. Piater and E. van Heerden, *J. Bacteriol.*, 2008, **190**, 3076–3082.
- 24 J. Bernard, E. van Heerden, I. W. C. E. Arends, D. J. Opperman and F. Hollmann, *ChemCatChem*, 2012, **4**, 196–199.
- 25 D. J. Opperman, B. T. Sewell, D. Lithauer, M. N. Isupov, J. A. Littlechild and E. van Heerden, *Biochem. Biophys. Res. Commun.*, 2010, **393**, 426–431.
- 26 S. Panke, M. G. Wubbolts, A. Schmid and B. Witholt, *Biotechnol. Bioeng.*, 2000, **69**, 91–100.
- 27 K. Otto, K. Hofstetter, M. Röthlisberger, B. Witholt and A. Schmid, *J. Bacteriol.*, 2004, **186**, 5292–5302.
- 28 V. Massey, *J. Biol. Chem.*, 1994, **269**, 22459–22462.
- 29 D. Holtmann and F. Hollmann, *ChemBioChem*, 2016, **17**, 1391–1398.
- 30 B. O. Burek, S. Bormann, F. Hollmann, J. Z. Bloh and D. Holtmann, *Green Chem.*, 2019, **21**, 3232–3249.
- 31 R. Ullrich, J. Nüske, K. Scheibner, J. Spantzel and M. Hofrichter, *Appl. Environ. Microbiol.*, 2004, **70**, 4575–4581.
- 32 P. Molina-Espeja, S. Ma, D. M. Mate, R. Ludwig and M. Alcalde, *Enzyme Microb. Technol.*, 2015, **73–74**, 29–33.
- 33 J. Ratzka, L. Lauterbach, O. Lenz and M. B. Ansorge-Schumacher, *J. Mol. Catal. B: Enzym.*, 2012, **74**, 219–223.
- 34 N. Herr, J. Ratzka, L. Lauterbach, O. Lenz and M. B. Ansorge-Schumacher, *J. Mol. Catal. B: Enzym.*, 2013, **97**, 169–174.
- 35 R. G. Keefe, M. J. Axley and A. L. Harabin, *Arch. Biochem. Biophys.*, 1995, **317**, 449–456.
- 36 Z. M. Shapiro and T. R. Moffette, *Hydrogen flamability data and application to PWR loss of coolant accident*, US Department of Energy, 1957, OSTI ID: 4327402.
- 37 A. Al-Shameri, M.-C. Petrich, K. junge Puring, U.-P. Apfel, B. M. Nestl and L. Lauterbach, *Angew. Chem., Int. Ed.*, 2020, **59**, 10929–10933.